ELSEVIER

International Journal of Mass Spectrometry 203 (2000) 59–69

International Journal of Mass Spectrometry

Determination of the metastable dissociation pathways for chromium/oxygen cluster ions sputtered from potassium chromate and dichromate using the ion-neutral correlation method

M.J. Van Stipdonk*, D.R. Justes[1], E.A. Schweikert

Department of Chemistry, Texas A&M University, P.O. Box 30012, College Station, TX 77843-3012, USA

Received 10 April 2000; accepted 9 June 2000

Abstract

Event-by-event bombardment and detection, coincidence counting, and the ion-neutral correlation method were used to study the dissociation of chromium/oxygen and chromium/oxygen/potassium cluster ions in the drift region of a reflectron time-of-flight (TOF) mass spectrometer. The cluster ions were sputtered from potassium chromate and dichromate by the impacts of ^{252}Cf fission fragments. The dissociation channel observed for the fragmentation of negative cluster ions was the emission of CrO_3^-. The positive secondary cluster ions decayed by shedding K^+. Decay fraction measurements were also performed to gain information about the relative stability to secondary ion dissociation and/or neutralization. (Int J Mass Spectrom 203 (2000) 59–69) © 2000 Elsevier Science B.V.

Keywords: Plasma desorption; Metastable dissociation; Cluster ions; Fragmentation pathways; Chromium

1. Introduction

A central theme of our research program has been to gain an understanding of secondary ion formation following energetic projectile impacts to facilitate the application of methods such as plasma desorption (PDMS) and secondary ion mass spectrometry (SIMS) to materials characterization and surface analysis. The accuracy with which a mass spectrum reflects the stoichiometry of the surface depends critically on how well the secondary ion species represent the relative abundance(s) and connection of elements and molecules within the solid. In order to determine how well secondary ions reflect surface composition, it is important to know the composition and structure of the secondary ion. For this reason, we have been developing and validating the ion-neutral correlation method as a tool to improve the accuracy of surface analysis by ion-induced desorption and time-of-flight (TOF) mass spectrometry, particularly as applied to inorganic materials. We recently described the application of the ion-neutral correlation method to elucidate the dissociation pathways of secondary ions sputtered from inorganic solids such as α-zirconium phosphate; lanthanum, bismuth and

* Corresponding author. Present address, Department of Chemistry, Wichita State University, Wichita, KS. E-mail: mjvansti@twsu.edu

[1] Present address, Department of Chemistry, Davey Laboratories, Pennsylvania State University, State College, PA.

PII S1387-3806(00)00264-5

calcium nitrate; and from sodium tetrafluoroborate by the impact of energetic primary ions [1–3]. Our methodology is based on the ion-neutral correlation method developed by Della Negra and Le Beyec [4,5] and has been applied to the determination of fragmentation pathways for organic and inorganic secondary ions sputtered from solid samples by keV and MeV energy primary ions [6–8]. Stated briefly, in this analytical approach event-by-event bombardment/detection and coincidence counting are used to identify fragment ions and neutral species that are correlated by virtue of arising from the metastable dissociation of the same precursor ion in the drift region of a reflectron TOF mass spectrometer. The ion-neutral correlation method is a unique way to obtain tandem or MS/MS data when using a reflectron TOF mass analyzer, and allows the metastable dissociation pathways for multiple precursor ions to be determined simultaneously under the same experimental conditions.

In this article we present the dissociation pathways discerned for positive and negative secondary ions sputtered from potassium chromate (K_2CrO_4) and dichromate ($K_2Cr_2O_7$) by ^{252}Cf fission fragment impacts as determined using the ion-neutral correlation method. In addition, decay fraction measurements were performed to determine the relative stability of the secondary ions to metastable decay and/or neutralization. These solids were the focus of these experiments due to the health risks associated with Cr(VI) in the form of particulates in the environment [9,10], and the interest in applying mass spectrometric techniques to the characterization and differentiation of Cr(III) and Cr(VI) solids such as the oxides, chromate, dichromate, nitrate, sulfate, and chloride using ion intensity patterns generated by laser desorption/ablation [11–14]. In addition, plasma desorption remains a viable method for generating secondary ion mass spectra from inorganic solids and to our knowledge the use of PDMS to speciate chromium/oxygen compounds has not yet been reported.

2. Experimental

The experiments described in this report were performed under event-by-event bombardment and detection conditions using a coincidence counting data collection protocol [15]. Positive and negative ion mass spectra of K_2CrO_4 and $K_2Cr_2O_7$ were collected using a reflectron TOF mass spectrometer built in-house: a detailed account of the configuration and operation has been provided elsewhere [2]. Briefly, the instrument includes a vacuum chamber housing a ^{252}Cf primary ion source (operated in transmission mode, with fission fragments passing through the target from the back side), a sample target-acceleration grid assembly, a 25-mm diameter microchannel plate (MCP) start detector and a 40-mm diameter reflected ion stop detector. An electrostatic ion mirror (or reflectron) is mounted to an extension connected to the vacuum chamber. Linear TOF mass spectra (or neutral spectra when voltage is applied to the mirror) are collected using a 40-mm MCP detector located behind the ion mirror. Positive and negative plasma desorption mass spectra of $K_2Cr_2O_7$ and K_2CrO_4 were acquired using an acceleration voltage of ± 8 kV. For reflected ion mass spectra and ion-neutral correlation metastable ion studies, a reflector voltage, V_r, of ± 8835 V (± 3 V) was used. This value was obtained by adjusting the mirror voltage until the highest resolving power for the sample specific peaks from *m/z* 100–300 was achieved ($\sim$2500 as $m/\Delta m$).

2.1. Sample target preparation

Sample supports for these experiments consisted of aluminized Mylar stretched over and glued to stainless steel aperture plates. Solid $K_2Cr_2O_7$ and K_2CrO_4 were purchased from Aldrich Chemical (St. Louis, MO) and used as received. Solutions of each were prepared by dissolving an appropriate amount of salt in distilled/deionized water to produce a concentration of .3 M. A 10 μL aliquot of $K_2Cr_2O_7$ or K_2CrO_4 solution was then mixed with 10 μL of a dilute solution of methylcellulose in distilled water, transferred to the Mylar substrate and allowed to dry under ambient conditions in a dark fume hood. The use of methylcellulose promotes wetting of the polymer support and induces thin, homogeneous surface coverage. The principal ion peaks observed from the methylcellulose additive are carbon and carbon/hy-

drogen cluster ions, are of low relative intensity, and do not interfere with the detection and mass assignment of peaks representative of either $K_2Cr_2O_7$ or K_2CrO_4. Past studies have also shown that the presence of methylcellulose does not inhibit the generation or detection of sample specific secondary ions [16].

2.2. Decay fraction and ion dissociation pathway studies

A decay fraction is a relative measure of the number of secondary ions that either dissociate to produce charged and neutral fragments, or in the case of negative secondary ions, undergo an electron detachment reaction in the drift region of the mass spectrometer. The decay fractions for secondary ions emitted from $K_2Cr_2O_7$ or K_2CrO_4 were measured by collecting two spectra each in the positive and negative ion modes. First, a linear TOF mass spectrum was acquired with an acceleration voltage $V_a = \pm 8.0$ kV and $V_r = 0$. The peaks in the linear TOF spectrum are an amalgam of intact ions and ion and neutral fragments from in-flight dissociation reactions. Next, a spectrum was acquired with $V_a = \pm 8.0$ kV and $V_r = 10.0$ kV, the latter voltage set to reject all ionized species. The linear TOF spectrum in this case provides a measure of the stop events corresponding to neutral species created by in-flight dissociation reactions. The decay fraction is calculated using the formula:

$$\text{Decay fraction} = I_{\text{neutrals}}/I_{\text{ions+neutrals}}$$

where I_{neutrals} corresponds to the peak area of a particular peak with V_r set to reject all ionized species (i.e. higher than V_a) and $I_{\text{ions+neutrals}}$ is the peak area of the same peak measured with the V_r set to 0 V. The net collection efficiency for the intact and fragment species for the range of cluster parent ions examined here is assumed to be the same. The stop counts, when operated in either the neutral only or the ions + neutrals mode, were not corrected for detector efficiency. The decay fractions, therefore, as calculated are not absolute and are considered "apparent" values that reflect the relative stability of different ions sputtered from the same sample.

The methodology for studying ion-neutral correlations from the metastable dissociation of secondary ions in a reflecting TOF instrument was developed by Della-Negra and Le Beyec [4,5]. Briefly, the ion and neutral fragments generated from discrete ion dissociation events can be separated using the electric field within an electrostatic mirror. The field will reflect secondary ions that remain intact, along with fragment ions from dissociation reactions. The neutral species from in-flight dissociation are not affected by the field and pass through the mirror to strike the direct detector. Due to conservation of momentum, the neutral from a particular precursor ion will have a linear flight time nearly equal to the precursor ion, and the neutral species flight time can be used to identify the dissociating ion.

To correlate the neutral and ion fragments that originate from the same dissociating ion, coincidence windows were set on a particular neutral peak detected using the MCP detector behind the electrostatic mirror. When setting the windows, we can discriminate between neutrals arising from in-flight dissociation and neutral species formed within the acceleration region: the latter are shifted to higher flight time according to the change in acceleration energy. The coincidence software registers correlated ion stop events at the reflected ion MCP detector within the entire 128 μs time-to-digital converter (TDC) acquisition time following its trigger by a fission fragment start signal. A coincidence spectrum is then obtained in which all of the stop events registered at the reflected detector are in coincidence with the start signal/fission fragment impact and the detection of the neutral species. The current software design allows up to 10 dissociation pathways to be monitored simultaneously.

3. Results and discussion

3.1. Negative and positive ion mass spectra

Fig. 1 shows the negative plasma desorption mass spectra generated from the KCr_2O_7 and $KCrO_4$ targets, respectively. The positive ion mass spectra

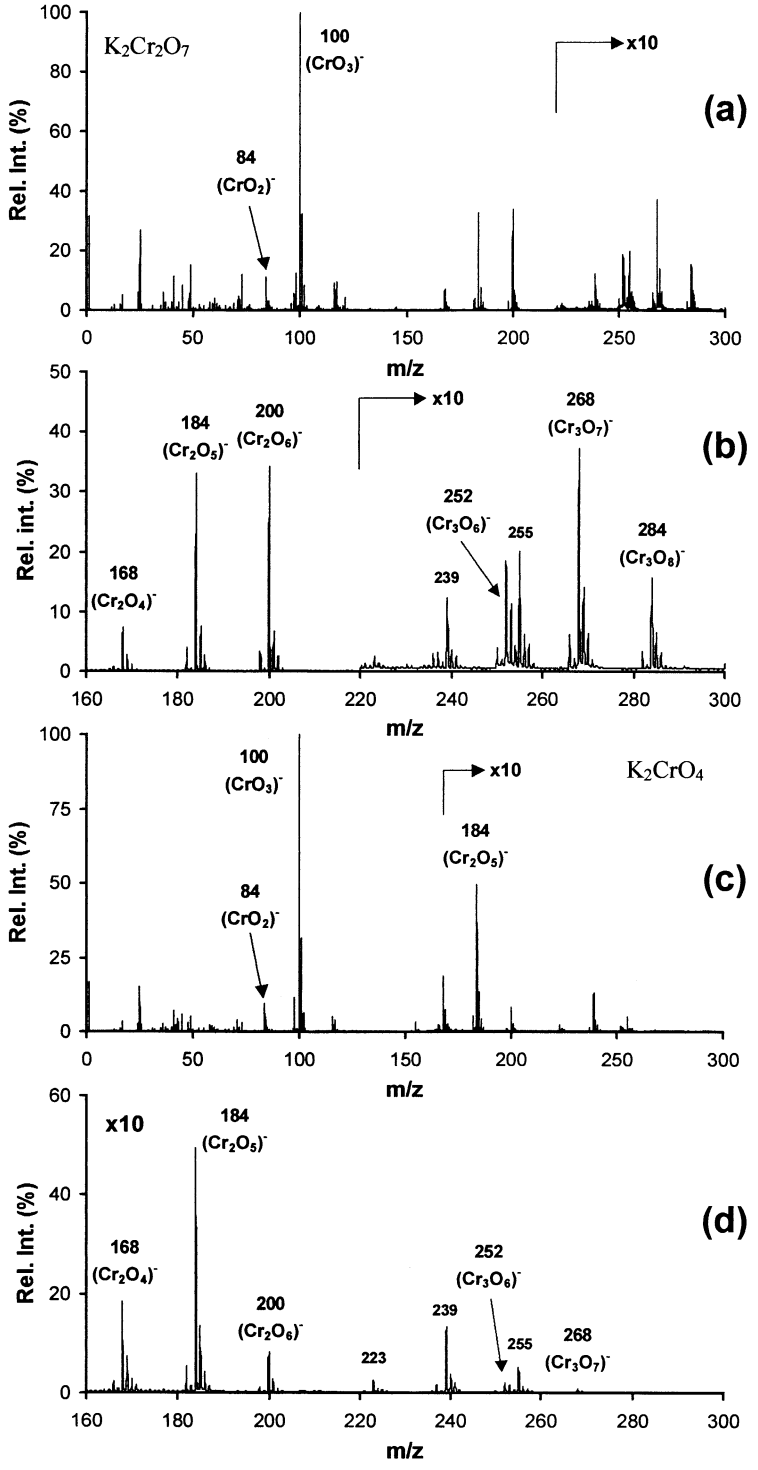

Fig. 1. Negative plasma desorption mass spectra of $K_2Cr_2O_7$ [(a) and (b)] and K_2CrO_4 [(c) and (d)]. The spectra in (b) and (d) are expanded views of the spectra in (a) and (c), provided to highlight the higher mass clusters ion emitted from both solids following MeV ion impacts.

produced from the same targets are shown in Fig. 2. The sample-specific secondary ions observed from both solids are summarized in Table 1. In general, the negative and positive ion plasma desorption spectra are similar, both in terms of secondary ion composition and intensity distribution, to the mass spectra produced from Cr/O solids by UV laser desorption (LD) [12,13]. As observed in the LD experiments, the majority of the secondary ions observed in the plasma desorption mass spectra are common to both $K_2Cr_2O_7$ and K_2CrO_4. There are, however, differences in the relative intensities and intensity distributions between the two solids as discussed below.

In the negative ion mode, the secondary cluster ion distribution extends to higher *m/z* values, and the relative intensities of the secondary ions are greater in the mass spectrum produced from $K_2Cr_2O_7$. The most prominent peak observed in both mass spectra is CrO_3^- at *m/z* 100, and the majority of the remaining sample-specific cluster ions are composed of Cr and O in varying proportions. The negative secondary ion peaks at *m/z* 223, 239, and 255 are separated by 16 mass units, corresponding to the sequential addition of O to the cluster composition. The molecular weights assigned to the three peaks, however, are not divisible solely into Cr and O constituents, and thus the cluster ions may also contain K. The peaks at *m/z* 223, 239, and 255 thus correspond to $\{KCr_2O_5^-\}$, $\{KCr_2O_6^-\}$, and $\{KCr_2O_7^-\}$, respectively. A change in the isotope pattern, characterized by an increase in intensity of the peak at $M + 2$ (where $M =$ the peaks at *m/z* 223, 239, and 255) due to the addition of ^{41}K is evidence that supports the inclusion of K to the composition of the ions at *m/z* 223, 239, and 255.

Of note in the negative ion mass spectra of K_2CrO_4 and $K_2Cr_2O_7$ are the differences in relative intensities of the secondary cluster ions at *m/z* 168 $\{Cr_2O_4^-\}$, 184 $\{Cr_2O_5^-\}$, and 200 $\{Cr_2O_6^-\}$, an observation expected due to the difference in stoichiometry between the chromate and dichromate salts. For instance, the intensity of $\{Cr_2O_6^-\}$ relative to $\{Cr_2O_5^-\}$ is higher in the spectrum produced from $K_2Cr_2O_7$. The relative intensity ratio $\{Cr_2O_6^-\}/\{Cr_2O_5^-\}$, .9 and .4 for dichromate and chromate, respectively, and the differences in relative intensity of the secondary ions greater than *m/z* 220 can be used to differentiate between the two solids. Relative ion intensity ratios, particularly for the secondary ions in the mass range between *m/z* 150 and 250, have been used to distinguish dichromate from chromate solids using LD mass spectrometry [12].

The most prominent peak in the positive ion mass spectra of $K_2Cr_2O_7$ and K_2CrO_4 is K^+ (*m/z* 39), followed by a prominent quartet of peaks at *m/z* 94–97. The compositions of these ions are assigned as $\{K_2O^+\}$ (*m/z* 94, 96) and $\{K_2OH^+\}$ (*m/z* 95, 97). We have also observed the formation of K/O cluster species following fission fragment impacts on solids such as KNO_3 and KIO_3 [17]. Three prominent positive secondary cluster ions were observed in the mass region between *m/z* 150 and 250 of the positive PDMS spectrum, corresponding to species composed of K, Cr, and O. The relative intensities of the peaks at *m/z* 178 $\{K_2CrO_3^+\}$, 217 $\{K_3CrO_3^+\}$, and 233 $\{K_3CrO_4^+\}$ are different for $K_2Cr_2O_7$ and K_2CrO_4, allowing differentiation between the two solids. As opposed to the negative ion mass spectra, the relative peak intensities in the positive mass spectra are higher in the mass spectrum produced from K_2CrO_4.

3.2. Secondary ion dissociation pathways

Coincidence windows were set on the neutral peaks from the dissociation of several prominent positive and negative secondary cluster ions observed in the mass spectra of $K_2Cr_2O_7$ and K_2CrO_4. To illustrate the coincidence spectra produced using the ion-neutral correlation protocol, Fig. 3 shows three negative ion mass spectra collected simultaneously from the same $K_2Cr_2O_7$ target, with the *x* axis expanded to highlight the flight-time region between 25 and 30 μs. Fig. 3(a) contains the total reflected ion mass spectrum, which is a sum of the reflected intact and fragment ions detected through the entire experimental run without discrimination by the use of coincidence windows. The spectra in Figs. 3(b) and 3(c) feature only the reflected intact and fragment ions observed in coincidence with the detection of the neutral species from the dissociation of $\{Cr_2O_5^-\}$ and $\{Cr_2O_6^-\}$ precursor ions, respectively. The fragment

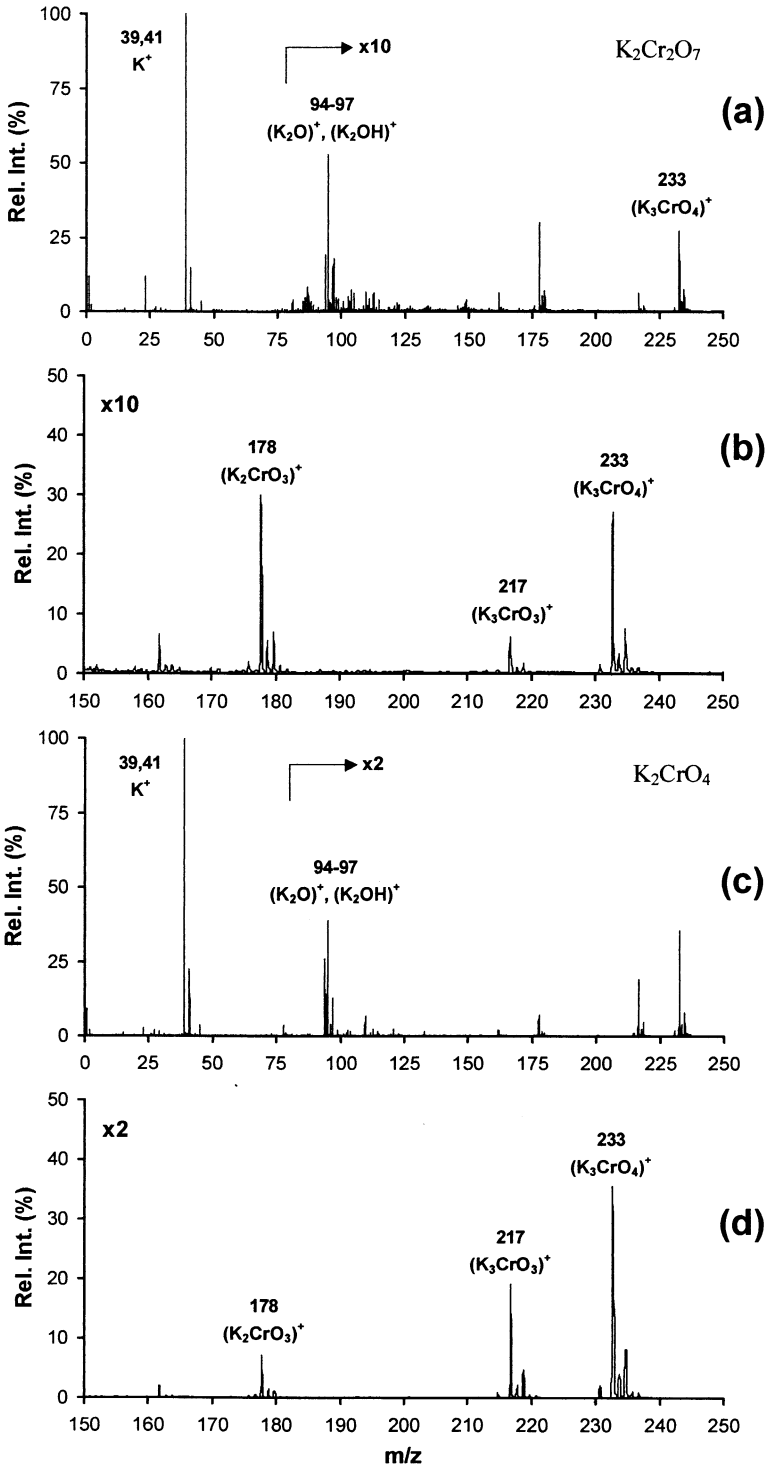

Fig. 2. Positive plasma desorption mass spectra of $K_2Cr_2O_7$ [(a) and (b)] and K_2CrO_4 [(c) and (d)]. The spectra in (b) and (d) are expanded views of the spectra in (a) and (c), provided to highlight the higher mass clusters ion emitted from both solids following MeV ion impacts.

Table 1
Sample specific secondary ions observed following ^{252}Cf fission fragment impacts on $K_2Cr_2O_7$ and K_2CrO_4.

Negative Ions	
CrO_2^-	84
CrO_3^-	100
$HCrO_4^-$	117
$Cr_2O_4^-$	168
$Cr_2O_5^-$	184
$Cr_2O_6^-$	200
$KCr_2O_5^-$	223
$KCr_2O_6^-$	239
$Cr_3O_6^-$	252
$KCr_2O_7^-$	255
$Cr_3O_7^-$	268
$Cr_3O_8^-$	284
Positive Ions	
K^+	39
K_2O^+	94
K_2OH^+	95
$K_2CrO_3^+$	178
$K_3CrO_3^+$	217
$K_3CrO_4^+$	233

ions from the dissociation reactions are identified by their characteristic broad peak shapes. The fragmentation pathways determined for each of the coincidence windows set in the positive and negative ion mass spectra are shown in Table 2. In some cases, the intensities of the neutral peaks were too low to accurately set the coincidence windows, prohibiting the determination of the dissociation pathways for certain precursor ions. The low intensities can be attributed to either a low overall emission yield of the precursor ion by ^{252}Cf fission fragment impacts, or to high stability in the gas phase (and hence low susceptibility to metastable dissociation on the timescale probed by our instrument). In addition, although prominent neutral peaks were observed, negatively charged fragment ions were not detected following the dissociation of several precursor ions—such was the case for the $\{Cr_2O_4^-\}$ ion. In this situation, the formation of the neutral species is assumed to be due to electron detachment reactions that lead to neutralization of the precursor ion.

The predominant dissociation pathway for the negative secondary ions was the emission of the stable CrO_3^- fragment ion. Assignment of the neutral species composition, as shown in Table 2, assumes that the dissociation reaction occurs by precursor ion "fission" into a fragment ion and neutral. We note, however, that the ion-neutral correlation method, as with many tandem and MS/MS approaches, does not directly probe the composition of the neutral species. For instance, the dissociation of the negative precursor ion at *m/z* 268, $\{Cr_3O_7^-\}$, will produce a CrO_3^- fragment ion and the neutral loss may correspond to either $Cr_2O_4^0$, or two CrO_2^0 units. It is clear from the metastable dissociation pathways that, in general, the negative cluster ions in the *m/z* range 150–300 are composed of the CrO_3 anion and small neutral units such as CrO_2, CrO_3, and Cr_2O_3. The prominence of the CrO_3^- fragment ion following metastable dissociation is not surprising because the same ion is the most prominent prompt fragment peak observed in the plasma desorption spectra of both K_2CrO_4 and $K_2Cr_2O_7$.

Of considerable interest in the negative ion dissociation pathway measurements was the secondary ion at *m/z* 239. The fragment ion for the dissociation reaction was CrO_3^-, leaving 139 u ($KCrO_3$) as the calculated mass of the neutral species. Assuming the neutral species is an intact unit, the dissociation pathway suggests that the composition assignment for the peak at *m/z* 239 should be $\{K(CrO_3)_2^-\}$, providing additional evidence of the inclusion of K within the cluster composition.

For each instance in which dissociation pathways could be determined, the positive secondary ions decayed by shedding K^+. The dissociation of the positive cluster ion at *m/z* 178 can be rationalized by the emission of K^+ and the ion pair formation between K^+ and CrO_3^-, the latter being the most prominent negatively charged ion emitted from either $K_2Cr_2O_4$ or K_2CrO_4. The dissociation of the cluster ion at *m/z* 233 produces K^+ and either a neutral composed of two K cations and a doubly charged CrO_4 unit, or two neutral species each composed of one K cation and a CrO_2 anion. The former combination is plausible based on the stability of the chromate (CrO_4^{-2}) anion and the fact that CrO_4^{2-}

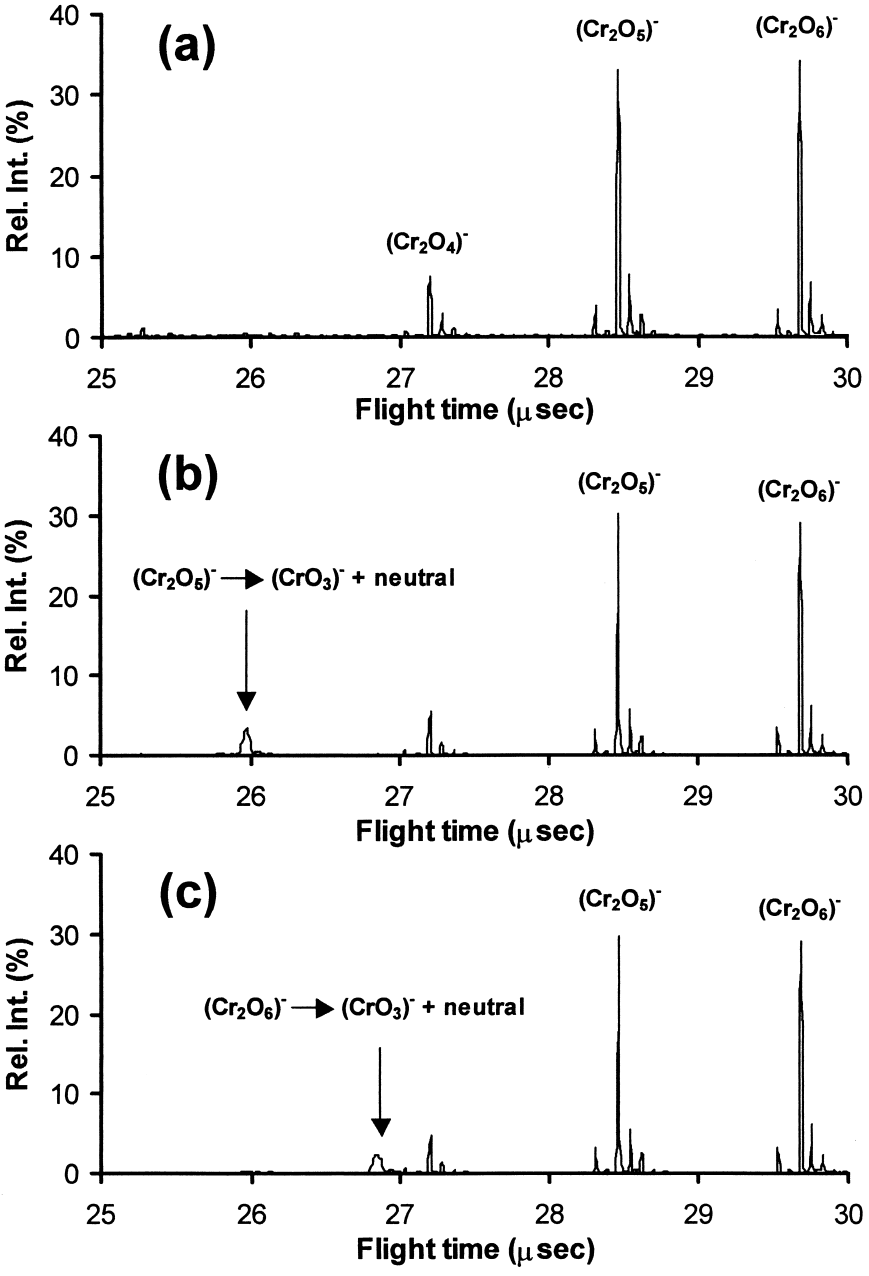

Fig. 3. Reflected ion mass spectra, highlighting the *m/z* region from 140–205, produced from $K_2Cr_2O_7$: (a) total reflected ion spectrum, (b) reflected ions observed in coincidence with the detection of the neutral from the dissociation of the $\{Cr_2O_5\}^-$ precursor ion, and (c) reflected ions observed in coincidence with the detection of the neutral from the dissociation of the $\{Cr_2O_6\}^-$ precursor ion. All three spectra were collected simultaneously, as described in the experimental section.

might be formed from dichromate ($Cr_2O_7^{2-}$) by breaking the bridging Cr–O–Cr bond. Because of the presence of the prompt CrO_2 fragment anion in the negative ion spectra of both solids, however, it is also possible that the positive cluster ion at *m/z* 233 is instead an aggregate of K^+ and CrO_2^- units.

Table 2
Dissociation pathways for negative and positive secondary cluster ions sputtered from $K_2Cr_2O_7$ and K_2CrO_4.

Negative Ions
$\{Cr_2O_5^-\} \Rightarrow CrO_3^- + CrO_2^0$
$\{Cr_2O_6^-\} \Rightarrow CrO_3^- + CrO_3^0$
$\{KCr_2O_6^-\} \Rightarrow CrO_3^- + KCrO_3^0$
$\{Cr_3O_6^-\} \Rightarrow CrO_3^- + Cr_2O_3^0$
$\{Cr_3O_7^-\} \Rightarrow CrO_3^- + Cr_2O_4^0$
Positive Ions
$\{K_2CrO_3^+\} \Rightarrow K^+ + KCrO_3^0$
$\{K_3CrO_3^+\} \Rightarrow K^+ + K_2CrO_3^0$
$\{K_3CrO_4^+\} \Rightarrow K^+ + K_2CrO_4^0$

3.3. Negative and positive ion decay fractions

As mentioned above, the apparent decay fraction provides a relative measure of the stability of secondary ions to unimolecular dissociation or electron detachment reactions in the drift region of the mass spectrometer. The decay fractions, calculated as explained in the experimental section, for the negative and positive sample-specific cluster ions emitted from $K_2Cr_2O_7$ are shown in Fig. 4. The decay fractions for the secondary ions emitted from K_2CrO_4 were identical to those for $K_2Cr_2O_7$ and thus are not shown in Fig. 4 for the sake of clarity.

In the negative ion mode, the decay fractions for CrO_2^- and CrO_3^- were less than .1, demonstrating the high stability of these secondary ions and low susceptibility to dissociation or neutralization reactions in the drift region of the instrument. The low decay fraction measured for CrO_3^- and the high intensity of this ion in the negative ion mass spectra of $K_2Cr_2O_7$ and K_2CrO_4 are evidence to support the assertion of a high electron affinity [19]. The $Cr_2O_4^-$ and $KCr_2O_6^-$ ions display high decay fractions, indicating that these secondary ions are less stable. Although a prominent neutral peak was observed, the coincidence spectrum for the dissociation of the $Cr_2O_4^-$ ion contained no fragment ion peak, suggesting that this precursor ion is unstable and decays by shedding an electron. It is not clear from these experiments whether the decay leads to $Cr_2O_4^0$ or two CrO_2^0 units. It is interesting to note that the stability of the secondary ions emitted from $K_2Cr_2O_7$ and K_2CrO_4 increases for species with a particular number of Cr constituents, as the number of O atoms increases. Although this observation may also be made by examining the relative ion intensity distributions in the mass spectrum (which in part are determined by ion stability), it is clearly demonstrated by the decrease in decay fraction value (assuming equal collection efficiencies during the decay fraction measurement). The high ion yields and low decay fractions can be rationalized, in part, by recognizing the stability of the +6 oxidation state of Cr, and the fact that the polyatomic ions with more oxygen represent a higher average Cr oxidation state within the precursor cluster.

In the positive ion mode, the decay fraction increases with the mass of the precursor ion, indicating a decrease in stability to metastable dissociation or neutralization with increasing size. Similar behavior has been noted for metal oxide [2], alkali halide [3], and van der Waals [18] cluster ions that dissociate in a reflecting TOF instrument.

4. Conclusions

The data presented here show that the secondary ion emission from $K_2Cr_2O_7$ and K_2CrO_4 stimulated by the impacts of ^{252}Cf fission fragments is sufficiently distinct to allow differentiation between the two solids. In this respect, plasma desorption provides analytical information similar to that obtained using LD mass spectrometry on analogous solids. Using the ion-neutral correlation method, we have determined the dissociation pathways for several negative and positive precursor ions sputtered from $K_2Cr_2O_7$ and K_2CrO_4 by the fission fragment projectiles. The main dissociation pathway for the negative ion species produces the CrO_3^- anion, whereas the only dissociation pathway observed for positive cluster ions is the emission of K^+. The dissociation pathways discerned for the negative ions indicate that the larger cluster ion species, those above *m/z* 150, are composed of CrO_3^- and neutral units that are not specific to either the chromate or dichromate salt. Therefore, the compositions and structures of these cluster ions do not

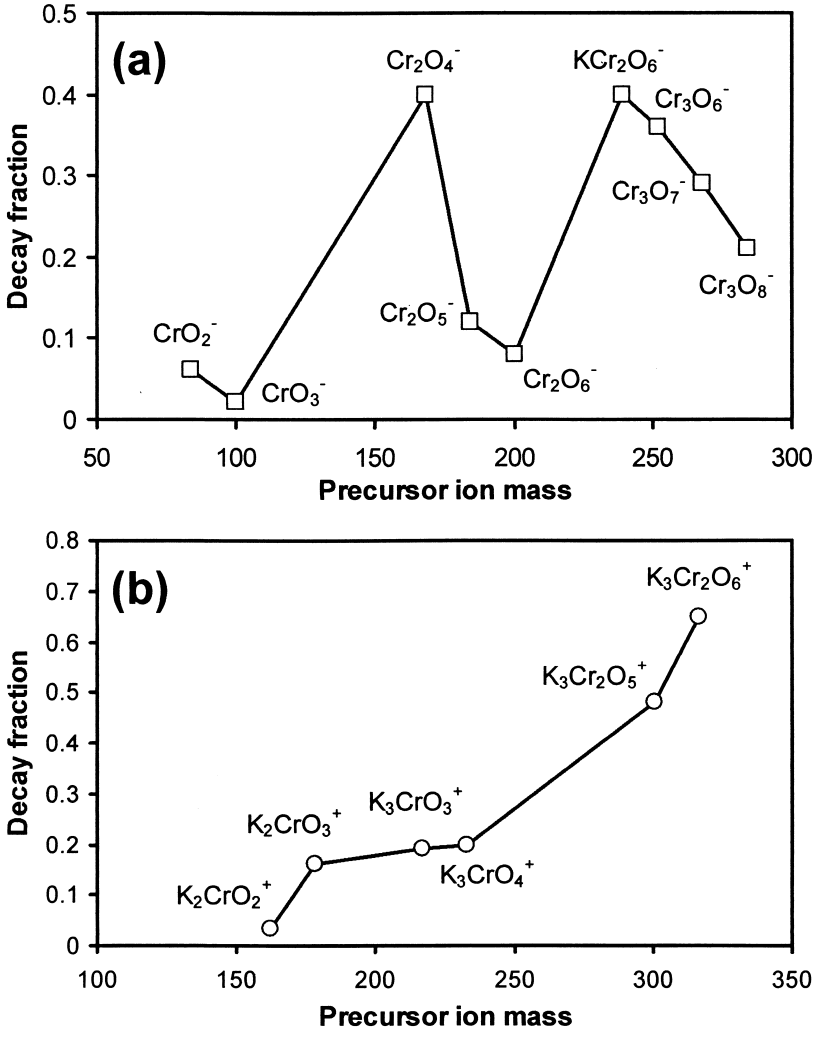

Fig. 4. Decay fractions for (a) negative and (b) positive secondary ions sputtered from $K_2Cr_2O_7$ by ^{252}Cf fission fragment projectiles. The decay fractions were calculated as described in the text. Negative and positive secondary ions of the same mass but sputtered from K_2CrO_4 had similar decay fractions.

necessarily reflect the true bonding pattern within the chromate and dichromate solids.

In a report describing the formation of similar chromium oxide cluster ions following LD of chromium/oxygen species in aerosols [13], Neubauer *et al.* discussed the possibility that the ion intensity distributions are influenced by the metastable dissociation of large cluster ions to produce smaller units such as CrO_2^- and CrO_3^-, particularly within the acceleration region of the mass spectrometer. One signature of dissociation in the acceleration region of a TOF mass spectrometer is a pronounced "tail" to the high mass (longer flight time) side of certain peaks that correspond to the ion products from metastable decay. No significant "tailing" to the high mass side of the CrO_2^- and CrO_3^- peaks was observed in the plasma desorption spectra of $K_2Cr_2O_7$ or K_2CrO_4 to indicate that pronounced fragmentation occurs within the acceleration region following ^{252}Cf fission fragment impacts. Our results do show, however, that several of the

polyatomic Cr/O ions sputtered by ^{252}Cf fission fragment impacts dissociate within the field free region of a mass spectrometer and that the major product ion is CrO_3^-. We note that metastable dissociation within the flight region was not observed in the LD experiments described in [13] though this may be due to differences in the dynamics and energetics between the LD and plasma desorption methods for ion generation. Though a detailed description of the mechanisms that underlie the generation of the ions from chromate and dichromate is not the focus of this report, the ion/ion and ion/molecule reactions that can occur in the high-density ablation plumes during laser desorption or ablation may not be operative to the same extent in plasma desorption. In any case, the metastable dissociation of the larger Cr/O cluster ions observed here supports the proposal that these species decay into smaller cluster ions such as CrO_3^- and as such our results support the idea that this fragmentation may contribute to the general ion abundance patterns observed following UV-laser desorption of chromium/oxygen solids.

Acknowledgements

This work was supported by the National Science Foundation (grant CHE-9727474). Assistance with the design and construction of the reflectron TOF instrument by R.D. English and E.F. da Silviera is also acknowledged.

References

[1] M.J. Van Stipdonk, E.A. Schweikert, Nucl. Instrum. Methods Phys. Res. B 112 (1996) 68.
[2] M.J. Van Stipdonk, D.R. Justes, R.D. English, E.A. Schweikert, J. Mass Spectrom. 34 (1999) 677.
[3] M.J. Van Stipdonk, W.R. Ferrell, D.R. Justes, R.D. English, E.A. Schweikert, Int. J. Mass Spectrom., in press.
[4] S. Della Negra, Y. LeBeyec, Anal. Chem. 57 (1985) 2036.
[5] A. Brunelle, S. Della Negra, J. Depauw, H. Joret, Y. Le Beyec, in Ion Formation from Organic Solids (IFOS V), A. Hedin, B.U.R. Sundqvist, A. Benninghoven (Eds.), Wiley, Chinchester, 1990, p. 39.
[6] S. Bouchonnet, J-P. Denhez, Y. Hoppilliard, C. Mauriac, Anal. Chem. 64 (1992) 742.
[7] X. Tang, R. Beavis, W. Ens, S. LaFortune, B. Schueler, K.G. Standing, Int. J. Mass Spectrom. Ion Processes 85 (1988) 43.
[8] X. Tang, W. Ens, K.G. Standing, J.B. Westmore, Anal. Chem. 60 (1988) 1791.
[9] P. Sen, M. Costa, Carcinogenesis 7 (1986) 1527.
[10] M. Sugiyama, X.W. Wang, M. Costa, Cancer Res. 46 (1986) 4547.
[11] A. Hachimi, E. Millon, J.F. Muller, E. Poitevin, Analusis 21 (1993) 77.
[12] A. Hachimi, E. Poitevin, G. Krier, J.F. Muller, M.F. Ruiz-Lopez, Int. J. Mass Spectrom. Ion Processes 144 (1995) 23.
[13] K.R. Neubauer, M.V. Johnston, A.S. Wexler, Int. J. Mass Spectrom. Ion Processes 151 (1995) 77.
[14] K. Poels, L. Van Vaeck, R. Gijbels, Anal. Chem. 70 (1998) 504.
[15] M.J. Van Stipdonk, E.A. Schweikert, M.A. Park, J. Mass Spectrom. 32 (1997) 1151.
[16] J.F. Blankenship, M.J. Van Stipdonk, E.A. Schweikert, Rapid Commun. Mass Spectrom. 11 (1997) 143.
[17] M.J. Van Stipdonk, E.A. Schweikert, unpublished results.
[18] S. Wei, A.W. Castleman Jr., Int. J. Mass Spectrom. Ion Processes 131 (1994) 233.
[19] D.L. Bricker, D.H. Russell, J. Am. Chem. Soc. 109 (1987) 3910.